J. Chem. Sci. (2021) 133:88
https://doi.org/10.1007/s12039-021-01956-9
© Indian Academy of Sciences

REGULAR ARTICLE

Special Issue on Beyond Classical Chemistry.

Selective turn-on sensing of fluoroquinolone drugs by zinc complexes of amide-based ligands

DIVYA PRABHA, DEVENDER SINGH and RAJEEV GUPTA*
Department of Chemistry, University of Delhi, Delhi 110 007, India
E-mail: rgupta@chemistry.du.ac.in

We dedicate this manuscript to the memory of late Prof. Bhaskar G. Maiya

MS received 20 March 2021; revised 23 May 2021; accepted 9 June 2021

Abstract. This work presents two mononuclear Zn(II) complexes of amide-based pincer ligands where migration of protons from the amidic N–H groups to the appended heterocyclic rings resulted in their protonation. The crystal structures of both the zinc complexes illustrated that such protonated heterocyclic rings created an H-bonding based secondary coordination sphere. Both complexes were utilized for the selective detection of fluoroquinolone antibiotics ciprofloxacin and norfloxacin. The two complexes exhibited high selectivity for norfloxacin with nanomolar detection limits of 290 and 460. The binding studies were further supported with the NMR spectroscopic and the molecular docking studies that exhibited that an antibiotic interacts with a zinc complex that was responsible for its emission enhancement based detection.

Keywords. Amide-based ligands; zinc complexes; fluorescent spectra; antibiotics; norfloxacin.

1. Introduction

Fluoroquinolones are a class of antibiotic drugs that have been extensively used to fight against several gram-positive and gram-negative bacteria.[1] Such drugs have attained therapeutic efficacy to treat urinary, gastrointestinal, gynaecological, ocular and skin infections while have also been successful in treating intra-abdominal infections.[2–4] Norfloxacin and ciprofloxacin are the emerging class of antibiotics that fall under the fluoroquinolone drugs (Figure 1).[5–7] Due to their widespread use, antibiotics as well as their residues are the major source of contamination for a wide range of environmental bodies including water and soil and are therefore a potential threat even at minimal concentrations.[8,9] Such a situation necessitates their monitoring in the environmental as well as in the biological samples. As a result, a wide range of methods and/or techniques have been developed for their detection such as spectrophotometry,[10] high-performance liquid chromatography,[11] capillary electrophoresis,[12] electrochemical analysis[13,14] and microbiological methods.[15] However, several such conventional methods and/or techniques not only require extensive instrumental setup but are also time-consuming and require a higher volume of organic solvents. In this context, fluorescence-based methods have received tremendous interest due to their better selectivity and sensitivity, easy visualization, on-site detection and fast response time.[16,17]

The incorporation of hydrogen bonds (H-bonds) in coordination complexes has attracted a great deal of attention in recent times.[18] This interest is inspired by the metalloenzymes and metalloproteins that use an array of H-bonds for not only modulating the substrate orientation but also controlling their activation.[18–20] As a result, many fascinating examples have been reported in the literature.[18–20] Our group has also provided several notable examples where H-bonds have been incorporated in the coordination complexes and such H-bonds have been found to assist in the substrate orientation as well as the substrate activation

*For correspondence

Supplementary Information: The online version contains supplementary material available at https://doi.org/10.1007/s12039-021-01956-9.

Published online: 19 August 2021

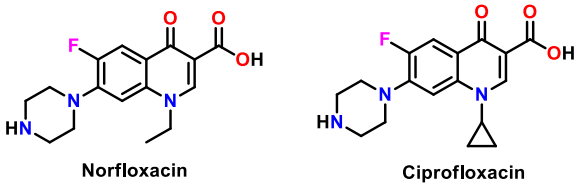

Figure 1. Chemical drawings of norfloxacin and ciprofloxacin.

strategies.[21–24] In such complexes, we have noticed that the insertion of a metal ion within the N_3 pincer cavity of pyridine-2,6-dicarboxamide based ligands containing appended heterocyclic rings resulted in the migration of amidic N-H groups to the appended heterocyclic rings.[21–24] As a result, such appended protonated heterocyclic rings create H-bonds in the vicinity of the metal ions and have assisted in controlling the substrate orientation adjacent to a metal ion.[21–24] In fact, we have also illustrated that H-bonds significantly influence the analyte detection.[25] In that context, coordination complexes offering strategically placed H-bonds may also assist in the detection of challenging analytes including antibiotics.

In this work, we have utilized two amide-based pincer ligands for the synthesis of their mononuclear Zn(II) complexes (Scheme 1). In both the complexes, migration of protons from the amidic N–H groups to the appended heterocyclic rings resulted in their protonation. Both complexes displayed the coordination of the Zn(II) ion within the N_3 pincer cavity while additionally ligated to the solvent molecules which were forming intramolecular H-bonds with the appended protonated heterocyclic rings. Both complexes have been utilized for the detection of fluoroquinolone based drugs, norfloxacin and ciprofloxacin, by the emission enhancement mechanism. Importantly, H-bonds have been suggested to assist in the binding and therefore detection of the antibiotics.

2. Experimental

2.1 *Chemicals*

All the chemicals and reagents used for the synthesis were of analytical grade and were used without further purification. The organic solvents were purified and dried according to the standard procedures. Ligands H_2L1 and H_2L2 were synthesized according to the procedure reported earlier.[22–24]

2.2 *Syntheses*

*2.2a Synthesis of [{L1(H)$_2$}Zn(H$_2$O)$_3$](ClO$_4$)$_2$ (**1**).* Ligand H_2L1 (0.1 g, 0.302 mmol) was dissolved in 3mL DMF to which $[Zn(H_2O)_6](ClO_4)_2$ (0.112 g, 0.303 mmol) was added as a solid under the magnetic

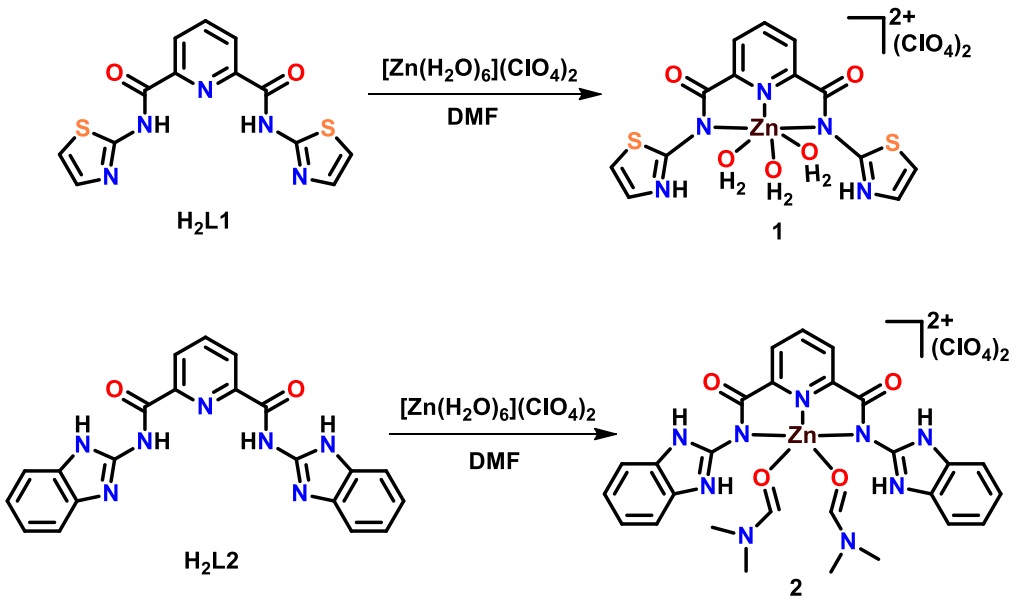

Scheme 1. Preparative route for the synthesis of Zn(II) complexes **1** and **2**.

stirring at room temperature. The stirring continued for 3 h. The solvent was then removed under the reduced pressure and the resulting oily remains were then treated with Et_2O to give pale yellow solid. Diffraction quality crystals were obtained by diffusing Et_2O to a CH_3CN solution of the crude product within 3 d. Yield 0.156 g (80%). Anal. Calcd. for $C_{13}H_{15}Cl_2N_5O_{13}S_2Zn$: C, 24.03; H, 2.33; N, 10.78; S, 9.87. Found: C, 24.19; H, 2.45; N, 10.70; S, 9.79. FTIR spectrum (Zn–Se ATR, cm^{-1}, selected peaks): 3309, 3225 (N–H), 1669 (C=O), 1070, 618 (Cl-O). ^{1}H NMR spectrum (400 MHz, DMSO-D_6): δ 13.35 (s, 2H), 8.42 (d, J = 8.4 Hz, 2H), 8.35–8.29 (m, 1H), 7.63 (d, J = 3.7 Hz, 2H), 7.37 (d, J = 4.3 Hz, 2H). ^{13}C NMR spectrum (100 MHz, DMSO-D_6): δ 162.76, 158.67, 148.25, 140.99, 138.81, 127.19, 115.07. Molar conductivity (MeCN, ca. 1 mM solution, 298 K) Λ_M: = 220 $\Omega^{-1}cm^2M^{-1}$. Absorption spectrum [λ max, nm, CH_3CN (ε, M^{-1} cm^{-1})]: 326 (345).

*2.2b Synthesis of [{L2(H)$_2$}Zn(DMF)$_2$](ClO$_4$)$_2$ (**2**).* Complex **2** was synthesized in a similar manner as explained for **1** using the following reagents: H_2L2 (0.1 g, 0.251 mmol) and $[Zn(H_2O)_6](ClO_4)_2$ (0.093 g, 0.250 mmol). Pale yellow crystalline compound was obtained on slow evaporation of the CH_3CN solution of crude product. Yield 0.158 g (79%). Anal. Calcd. for $C_{27}H_{29}Cl_2N_9O_{12}Zn$: C, 40.14; H, 3.62; N, 15.60. Found: C, 40.28; H, 3.54; N, 15.76. FTIR spectrum (Zn–Se ATR, cm^{-1}, selected peaks): 3331, 3241 (N–H), 1652 (C=O), 1067, 617 (Cl-O). ^{1}H NMR (400 MHz, DMSO-D_6): δ 12.90 (s, 2H), 8.52 (d, J = 7.7 Hz, 2H), 8.40 (t, J = 7.7 Hz, 1H), 7.95 (s, 1H), 7.58 (d, J = 8.9 Hz, 4H), 7.19 (d, J = 5.8 Hz, 4H). ^{13}C NMR spectrum (100 MHz, DMSO-D_6): δ 163.39, 162.95, 148.24, 146.49, 140.96, 139.19, 126.97, 122.05. Molar conductivity (MeCN, ca. 1 mM solution, 298 K) Λ_M: = 230 $\Omega^{-1}cm^2M^{-1}$. Absorption spectrum [λ max, nm, CH_3CN (ε, M^{-1} cm^{-1})]: 323 (545).

2.3 *Physical methods*

Elemental analysis data were obtained from the Elementar Analysen Systeme GmbH Vario EL-III instrument. The conductivity measurements were done with Eutech (model number: CON-510) digital conductivity bridge. The ^{1}H and ^{13}C NMR spectra were recorded with a JEOL 400 MHz instrument. FTIR spectra (Zn–Se ATR) were recorded with a PerkinElmer Spectrum-Two spectrometer. The absorption spectra were obtained with a Perkin-Elmer Lambda–950 spectrophotometer. Fluorescence spectral studies were carried out with a Cary Eclipse fluorescence spectrophotometer.

2.4 *X-ray crystallography*

The intensity data for complexes **1**–**2** were collected at 298 K with an Oxford XCalibur CCD diffractometer using graphite mono-chromated Mo-Kα radiation (λ = 0.71073 Å).[26] The structures were solved by direct methods using SIR-92 program[27] and refined by the full-matrix least-square refinement techniques on F^2 using SHELXL-2014/7.[28] The hydrogen atoms were placed at the calculated positions and included in the last cycles of the refinement whereas non-hydrogen atoms were refined anisotropically. All calculations were performed using WinGX crystallographic software package 70.[29] The crystallographic data collection and structure solution parameters are summarized in Table 1 whereas detailed bonding parameters are collected in Table S1 (Supplementary Information).

2.5 *Spectral studies and determination of detection limit and binding constants*

HPLC grade solvents were used for the absorption and emission spectral measurements. Stock solution of complexes **1** and **2** were prepared in CH_3CN. For the detection of antibiotics; stock solution of furazolidone, nitrofurazone, nitrofurantoin, amoxicillin, penicillin, ornidazole, azithromycin, isoniazid, norfloxacin and ciprofloxacin were prepared in EtOH. All UV-Visible and fluorescence spectral experiments were performed with a 1.0 cm path length cuvette at 25 °C. All absorption and emission spectral studies involving zinc complexes were done in EtOH containing 2% CH_3CN. Detection limit[30–33] was calculated using equation (1) where σ is the standard deviation of ten blank emission measurements of complexes **1** and **2** and k is the slope of a plot of emission of complexes **1** and **2** versus [antibiotic]. The binding constant (K_b) was determined from the ratio of intercept and slope of the straight line from the Benesi-Hildebrand plot[34] of $1/(I-I_0)$ against 1/[antibiotic] (equation 2) where I_0 and I are the emissions of complexes **1** and **2** in the absence and in the presence of antibiotic, respectively and I_{min} is the minimum emission in the presence of an antibiotic.

Detection limit:

$$3\sigma/k \tag{1}$$

$$1/(I - I_0) = 1/\{K_b(I_0 - I_{min})[\text{ antibiotic}]\} + 1/(I_0 - I_{min}) \tag{2}$$

Table 1. Crystallographic data collection and structure refinement parameters for **1** and **2**.

Compound	**1**	**2**
Formula	$C_{13}H_{14}Cl_2N_5O_{13}S_2Zn$	$C_{27}H_{27}Cl_2N_9O_{12}Zn$
Formula weight	648.68	805.87
T (K)	298(2)	298(2)
System	Monoclinic	Monoclinic
Space group	*I2/a*	$P2_1/c$
a (Å)	14.9688(5)	9.2679(6)
b (Å)	11.9500(7)	24.161
c (Å)	13.403	14.705(4)
α (°)	90	90
β (°)	96.10	95.80
γ (°)	90	90
V (Å^3)	2383.94(16)	3275.9(9)
Z	4	4
ρ calc (mg/m^3)	1.807	1.634
μ (mm^{-1})	1.503	0.990
F (000)	1308	1648
Goodness-of-fit (GOF) on F^2	1.031	1.069
Final *R* indices $[I > 2\sigma(I)]^{a,b}$	R_1 = 0.0378, wR_2 = 0.1031	R_1 = 0.0624, wR_2 = 0.1599
R indices (all data)	R_1 = 0.0467, wR_2 = 0.1105	R_1 = 0.0678, wR_2 = 0.1640
Largest diff. peak and hole (e.Å^{-3})	0.657 and -0.425	1.942 and -1.471
CCDC No.	2071653	2071654

[aa]$R = \sum(||Fo| - |Fc||)/\sum|Fo|$,

[b]$wR = \left\{\sum\left[w\left(F_o^2 - F_c^2\right)^2\right]/\sum\left[w\left(F_o^2\right)^2\right]\right\}^{1/2}$

3. Results and Discussion

3.1 *Syntheses and characterization of Zn(II) complexes 1-2*

Ligands H_2L1 and H_2L2 were selected for the synthesis of their Zn(II) complexes as they are known to form H-bonds in the vicinity of the metal ion coordinated within the N_3 pincer cavity.[22–24] Mononuclear Zn(II) complexes **1** and **2** with the formula $[Zn\{L(H)_2\}](ClO_4)_2$ were prepared by treating the corresponding ligands with $[Zn(H_2O)_6](ClO_4)_2$ in the absence of any base. Both complexes were obtained as the pale yellow crystalline products after standard workup followed by crystallization. Importantly, both complexes displayed the migration of protons from the amidic N-H groups to the pendant heterocyclic rings; thiazole in **1** and benzimidazole in **2**. FTIR spectra exhibited hypsochromically shifted $\nu_{N\text{-}H}$ stretches at 3309 and 3225 cm^{-1} for **1** and at 3331 and 3241 cm^{-1} for **2**, respectively. Similarly, red-shifted $\nu_{c=o}$ stretches at 1669 and 1652 cm^{-1} for **1** and **2** from their respective ligands confirmed proton migration and the involvement of deprotonated $N_{amidate}$ groups in bonding (Figure S1, SI).[35,36] A broad vibration near 1070 cm^{-1} and a strong and sharp band near 620 cm^{-1} illustrated the presence of ionic perchlorate.[35,36] Both complexes were further characterized by the ^{1}H and ^{13}C NMR spectra (Figures S2–S5, SI). In the proton NMR spectra, a singlet at δ 13.35 for **1** and 12.90 for **2** corresponded to the protonated heterocyclic ring N–H protons (Figure 2). The proton NMR spectra for both the complexes further displayed ring protons between 7–9 ppm. The ^{13}C NMR spectra for two complexes displayed assorted ring as well as carbonyl resonances at their respective positions. Conductivity measurements supported a 1:2 electrolytic nature for both the complexes.[37] Absorption spectra for both the Zn(II) complexes (conc. ca. 20 μM) exhibited bands at 330 nm which are tentatively assigned to ligand-centred π–π* and/or n–π* transitions (Figure S6, SI). To investigate the emission characteristics of the Zn(II) complexes; emission and excitation spectra were measured (Figures S7 and S8, SI).[38–40] Both complexes **1** and **2** illustrated a very weak emission maximum at 430 nm under excitation wavelength at 330 nm and both the complexes showed excitation maximum at 330 nm.

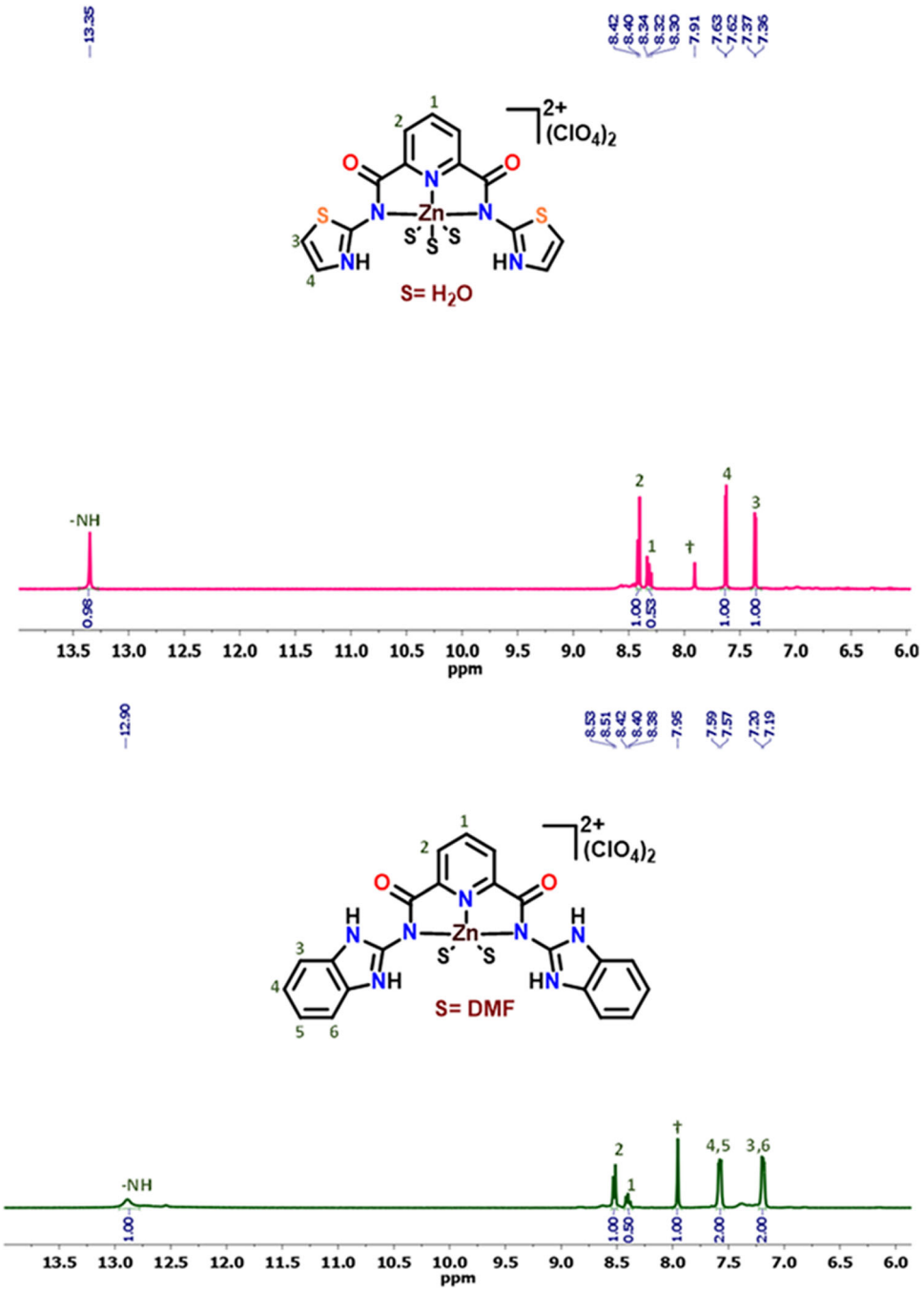

Figure 2. ^{1}H NMR spectra of complexes **1** (pink trace) and **2** (green trace) recorded in DMSO-d_6 where † represents –C(O)H proton of the DMF molecule(s).

3.2 *Crystal structures*

Both the complexes were crystallographically characterized (Table 1) and their molecular structures are shown in Figure 3 whereas selected bonding parameters are given in Table S1 (supplementary information). The crystal structures exhibited the presence of Zn(II) ion within the N_3 pincer cavity of the ligand bonded to two deprotonated anionic $N_{amidate}$ groups and one neutral $N_{pyridyl}$ atom.[41,42] Typical for pyridine-2,6-dicarboxamide based scaffolds, the Zn-N_{amide} bond lengths were longer than that of Zn-$N_{pyridyl}$ ones.[23,43,44] The geometry around the Zn^{2+} ion in complex **1** can be best described as the distorted octahedral with 2-fold axis passing through the atoms C1, N1, Zn and O3. The geometry in complex **2** is distorted square-pyramidal with τ distortion parameter of 0.373.[45] For a perfect square-pyramidal and a perfect trigonal-bipyramidal geometry, the ideal value of τ_5 is 0 and 1, respectively.[45] In both complexes, the

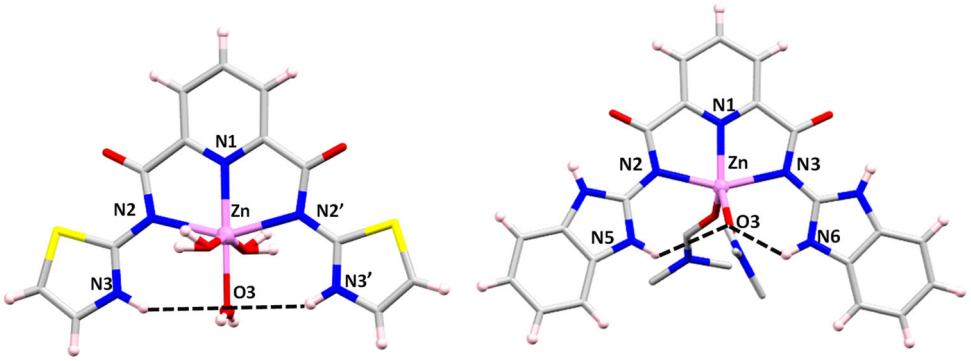

Figure 3. Crystal structures of zinc complexes **1** and **2**. Thermal ellipsoids are drawn at 30% probability level whereas perchlorate ions are not shown for clarity. Selected bond distances for complex **1**: Zn-N1, 2.062(3); Zn-N2, 2.2377(18); Zn-O2, 2.0870(17); Zn-O3, 2.132(3). Selected bond distances for complex **2**: Zn-N1, 2.013(3); Zn-N2, 2.148(3); Zn-N3, 2.143(3); Zn-O3, 1.967(3); Zn-O4, 1.988(3). See Table S1 (supplementary information) for other bonding parameters.

pendant heterocyclic rings were protonated due to the migration of protons.[46,47] As a result, such protonated heterocyclic rings formed H-bonds to the coordinated water molecule in the basal plane in case of **1** and coordinated DMF molecules in **2** (Tables S2 and S3, SI). In complex **1**, the heterocycle-NH···OH_2 H-bonding synthon displayed heteroatom separation of 3.262 Å. Similarly, heterocycle-NH···O_{DMF} separations in complex **2** were in the range of 3.159-3.184 Å. Such H-bonding separations indicated the existence of moderately strong intramolecular H-bonding in both the complexes.[46,47] An interesting consequence of H-bonding in the secondary coordination sphere is that they may orient incoming substrates and enhance the detection capability of the zinc complexes. The perchlorate ions in the crystal lattice were involved in the H-bonding interactions therefore connected cationic complexes together (Figures S9 and S10, SI).

3.3 *Detection of antibiotics*

3.3a *Detection and binding studies*: Complexes **1** and **2** offered Zn(II) ions containing labile solvent molecules and the presence of H-bonds in the vicinity of the metal ion.[21–24] While the presence of labile sites suggested that they could potentially create vacant site(s) for a suitable analyte to interact with; the H-bonding groups provided an opportunity for them to interact with an analyte.[48,49] In this context, antibiotics offer exciting detection opportunities as they offer many functional groups that could either interact with a metal ion or form H-bonds with suitable donors/acceptors. Therefore, both complexes **1** and **2** were investigated for their potential interaction with the assorted antibiotics.[50] On excitation at 350 nm, complexes **1** and **2** exhibited very weak emission centred at 430 nm. However, prominent emission spectral changes were noted on the addition of different antibiotics to the solution of **1** and **2** as shown in Figures 4a and 4b. Among different antibiotics, notable spectral changes were observed for fluoroquinolones. Notably, the addition of norfloxacin caused the maximum emission enhancement followed by ciprofloxacin whereas other antibiotics such as furazolidone, nitrofurazone, nitrofurantoin, amoxicillin, penicillin, ornidazole, azithromycin and isoniazid did not significantly perturb the emission spectral intensities of **1** and **2**. A comparison by the bar diagram for complexes **1** and **2** (Figure 4c) clearly illustrate that norfloxacin exhibited maximum emission enhancement followed by ciprofloxacin compared to the remaining antibiotics.

Notably, both norfloxacin and ciprofloxacin are themselves florescent (see Figure S11, SI for their absorption and excitation spectra); however, their complexation with Zn(II) complexes significantly enhanced the fluorescence of the [Zn-complex-antibiotic] adduct (Figure 5).[50] Figure S12, SI displays that the emission intensity for the [Zn-complex-antibiotic] adduct, formed between a zinc complex and an antibiotic, was maximum when the excitation wavelength was 350 nm when compared to other wavelengths (300–360 nm). As a result, all emission spectral titrations were performed at 350 nm excitation wavelength. Although emission spectral enhancement results were somewhat similar for both norfloxacin and ciprofloxacin but we focussed on norfloxacin due to its greater emission enhancement. Considering the florescent nature of norfloxacin,[51] the effect of variable concentration of norfloxacin (0-50 μM) on the fixed concentration of complexes **1** and **2** (20 μM) (Figure 6; Figures S13 and S14, SI) as well as the effect of

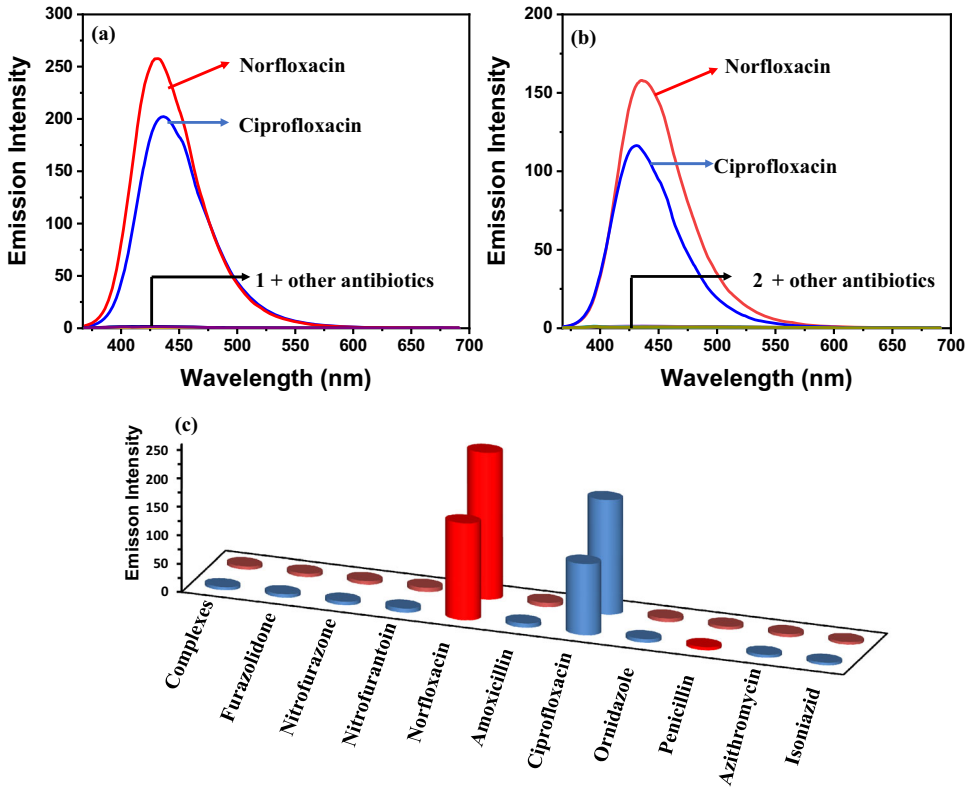

Figure 4. Change in the emission spectra of complexes (20 μM) (a) **1** and (b) **2** in the presence of 5 equiv. of different antibiotics. (c) Bar diagram showing emission spectral enhancement for zinc complexes in the presence of different antibiotics: **1** (430 nm, red bars) and **2** (430 nm, blue bars). All studies were performed in EtOH containing 2% CH_3CN (λ_{ex} = 350 nm).

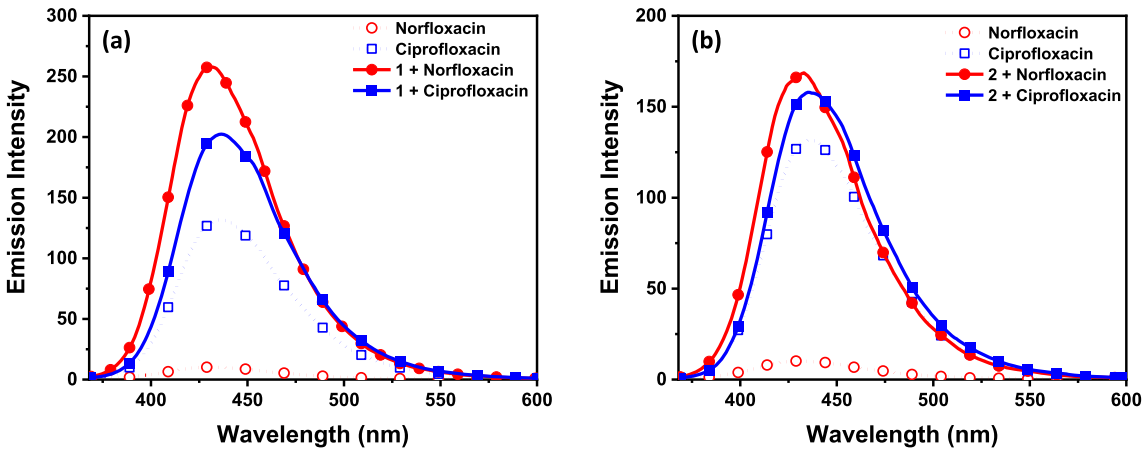

Figure 5. Comparative emission spectra of complexes (a) **1** and (b) **2** with ciprofloxacin and norfloxacin. All studies were performed in EtOH containing 2% CH_3CN (λ_{ex} = 350 nm).

variable concentration of Zn(II) complexes (0-20 μM) on the fixed concentration of norfloxacin (50 μM) were studied (Figures S15 and S16, SI). In both cases, significant 'turn-on' emission was observed as a result of the formation of [Zn-complex-antibiotic] adduct. From the concentration variation plots, the extent of binding was evaluated by the determination of detection limits and binding constants (K_b) (Table 2).[52–54] Both complexes **1** and **2** exhibited notable detection limits of 0.29 and 0.46 μM, respectively as well as high binding constants as presented in Table 2.

3.3b *Selectivity studies*: For many practical applications, analyte selectivity is an important factor for any chemosensor.[51–54] Therefore, selectivity for the recognition of norfloxacin from assorted

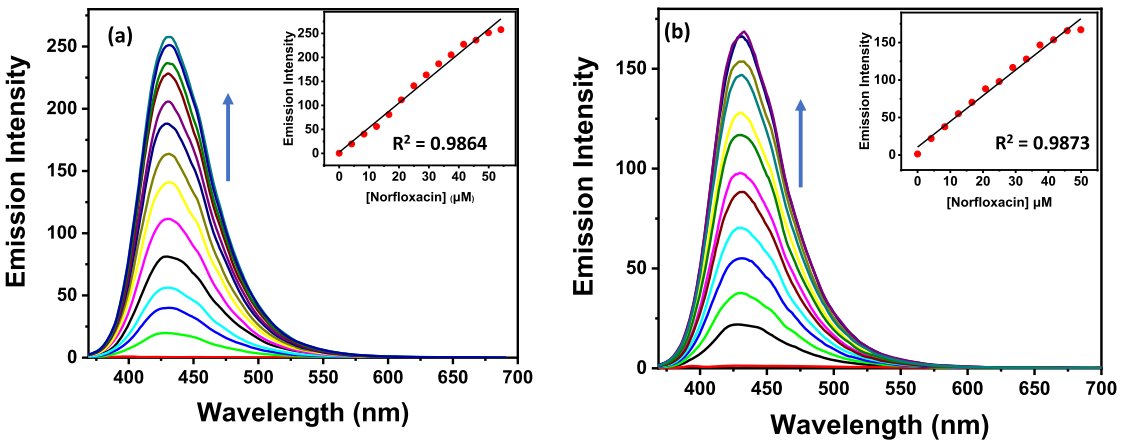

Figure 6. Change in the emission spectra of zinc complexes (20 μM) (a) **1** and (b) **2** after the successive addition of norfloxacin (0-50 μM). All studies were performed in EtOH containing 2% CH_3CN (λ_{ex} = 350 nm).

Table 2. Detection limit (DL) and binding constant (K_b) for the detection of norfloxacin by zinc complexes **1** and **2** by using emission spectroscopy.

Complex	DL (μM)	K_b $(M^{-1})^a$	K_b $(M^{-1})^b$
1	0.29	0.39 x 10^4	0.34 x 10^4
2	0.46	1.13 x 10^4	1.70 x 10^4

[a]Fixed concentration of zinc complexes while increasing the concentration of norfloxacin. [b]Fixed concentration of norfloxacin while increasing the concentration of zinc complexes.

antibiotics was investigated both for complexes **1** and **2** (Figure 7). The selectivity studies were investigated by carrying out the competitive binding analysis of norfloxacin in presence of equimolar concentration of other antibiotics.[51–54] Importantly, no notable change in the emission spectral intensities of complexes **1** and **2** in the presence of norfloxacin was observed in the presence of other antibiotics; furazolidone, nitrofurazone, nitrofurantoin, amoxicillin, penicillin, ornidazole, azithromycin and isoniazid as shown in Figures 7a and 7b. It can therefore be asserted that the present Zn(II) complexes are highly selective towards norfloxacin even in the presence of other assorted antibiotics.

3.4 *Mode of binding*

The emission spectral studies suggested significant interaction between complexes **1** and **2** to that of norfloxacin. Subsequently, Job's plot[51–54] was used for finding out the stoichiometry of norfloxacin to that of a zinc complex (Figure 8). From these studies, a 1:1 stoichiometry between norfloxacin and zinc complexes was obtained. The 1:1 stoichiometry was further supported by the Benesi-Hildebrand plots that showed a straight line for a 1:1 stoichiometry between norfloxacin and a zinc complex (Figures S13 and S16, SI).[51–54] On the other hand, an attempted 1:2 stoichiometry between the Zn(II) complexes and

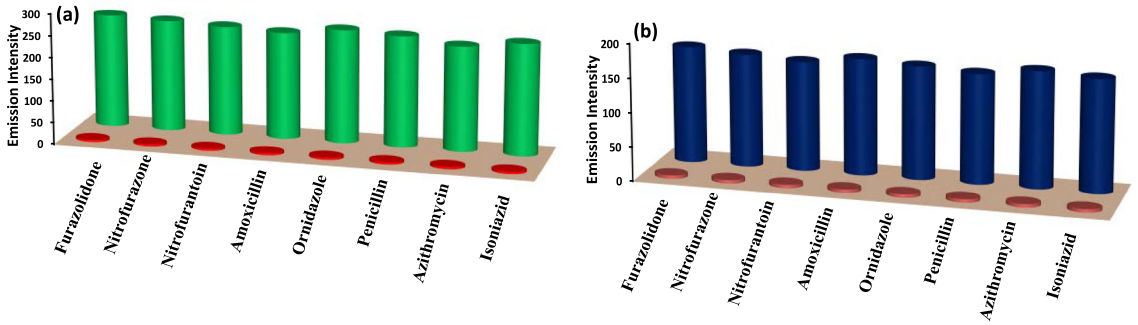

Figure 7. Selectivity for complexes (a) **1** + other antibiotics (red pillars); **1** + other antibiotics + norfloxacin (green pillars) and (b) **2** + other antibiotics (brown pillars); **2** + other antibiotics + norfloxacin (blue pillars). All studies were performed in EtOH containing 2% CH_3CN.

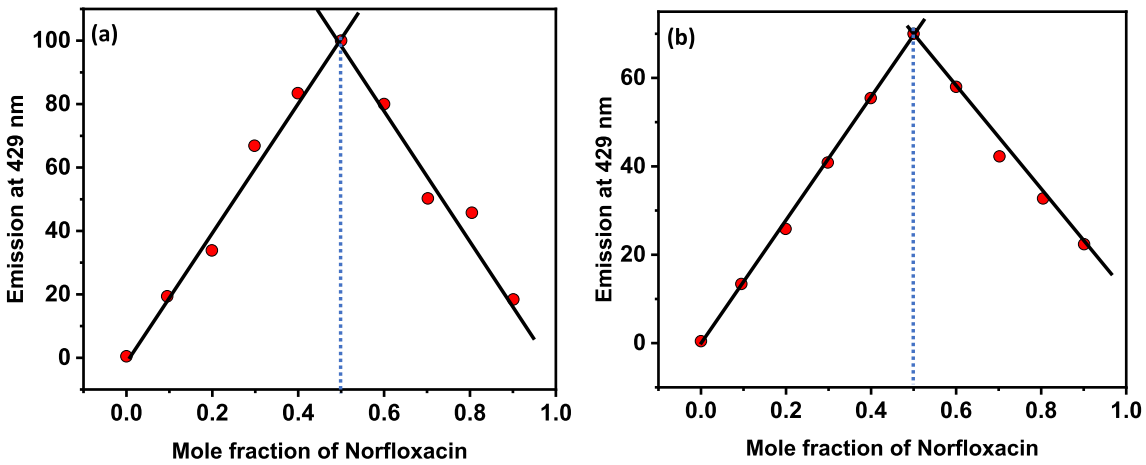

Figure 8. Job's plot for the detection of norfloxacin by complexes (a) **1** and (b) **2** in EtOH containing 2% CH_3CN.

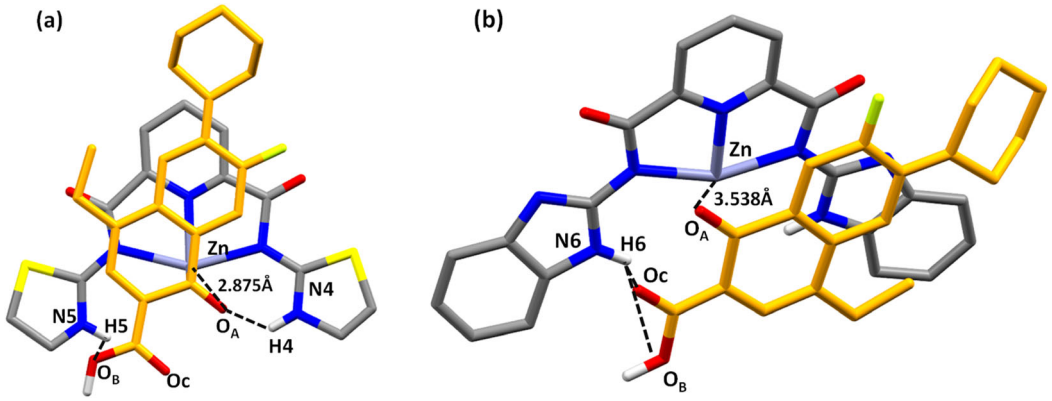

Figure 9. Molecular docking structures of complexes **1** and **2** with norfloxacin (shown in golden color for distinction except O and F atoms). The O_A atom of norfloxacin was found to coordinate with the Zn(II) ion while both protonated thiazolium and benzimidazolium rings were involved in the H-bonding interactions (N5-H5…O_B: 2.805 Å) and (N4-H4…O_A: 3.473 Å) in **1** and (N6-H6…O_B: 3.506 Å) and (N6-H6…O_c: 3.241 Å) in **2**. Only N-H protons of heterocyclic rings and H_{COOH} are shown for clarity.

norfloxacin showed significant deviation from the straight line (Figure S14, SI). Such a fact further point towards a 1:1 stoichiometry between a Zn(II) complex and norfloxacin.

In order to support analyte binding, molecular docking studies[55,56] for both the complexes with norfloxacin were performed (Figure 9). The molecular docked structure of norfloxacin with complexes **1** and **2** showed that O_A atom of the drug was found to coordinate with the Zn(II) ion with bond distances of 2.875 Å and 3.538 Å, respectively. In addition, protonated heterocyclic rings were involved in the H-bonding interactions both with the O_A and O_B atoms of norfloxacin in case of **1**. These interactions were further strengthened by the π…π stacking between the pyridine ring of the complex to that of benzene ring of norfloxacin with a center-to-center separation of 2.901 Å in **1**. Complex **2** also showed similar types of H-bonding interactions as illustrated in Figure 9b.

The molecular docking studies were further supported by recording ^{1}H NMR spectrum of a mixture of complex **1** and norfloxacin. As the molecular docking showed that C=O and COOH functional groups along with the benzene ring of norfloxacin were involved in multiple interactions with the zinc complex; ^{1}H NMR spectrum clearly justified the same. In comparison with the proton NMR spectrum of norfloxacin, [complex-drug] mixture exhibited notable red-shifts for the benzene ring protons (Figure S17, SI). Similarly, N-H protons of the protonated thiazolium rings were found to shift from 13.34 to 13.36 ppm, indicating their involvement in interactions with the norfloxacin

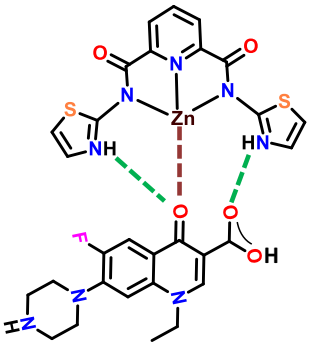

Figure 10. Schematic illustration explaining the mode of interaction between the Zn(II) complex **1** and norfloxacin responsible for the emission enhancement led detection. Brown and green dots respectively represent coordination bonding and H-bonding.

(Figure S18, SI). Collectively, emission spectral enhancement is attributed to the synergistic interactions involving Zn-O_{drug} coordination as well as H-bonding and π…π interactions between the zinc complex and norfloxacin as shown in Figure 10.[57]

4. Conclusions

This work has presented the synthesis and characterization of novel pincer-cavity based zinc complexes offering intramolecular H-bonding functional groups. Such zinc complexes functioned as the fluorescent chemosensors for the selective detection of fluoroquinolone drugs, norfloxacin and ciprofloxacin, and particularly norfloxacin. The detailed emission spectral titrations, binding studies, Job's plots, detection limits and molecular docking studies substantiated notable interactions of the zinc complexes to that of norfloxacin *via* coordination, H-bonding and π…π interactions. It is noteworthy to mention that the present zinc complexes not only exhibited high selectivity and sensitivity but also involved well-positioned H-bonds for the exclusive detection of antibiotics. The present work is notable in illustrating that simple coordination complexes could be utilized for the detection of challenging analytes such as antibiotics.[50] Our future work is focused on using the present zinc complexes in removing traces of antibiotics from contaminated sources.[58,59]

Supplementary Information (SI)

Figures S1–S18 and Tables S1–S3 are available at www.ias.ac.in/chemsci.

Acknowledgements

RG acknowledges financial assistance from the Council of Scientific and Industrial Research, New Delhi (01(2841)/16/EMR-II) and IoE project from the University of Delhi. DP thanks UGC, New Delhi for her fellowship. DS thanks CSIR, New Delhi for his fellowship. Authors thank CIF-USIC at this university for the instrumental facilities including X-ray data collection.

References

1. Lavaee P, Danesh NM, Ramezani M, Abnous K and Taghdisi SM 2017 Colorimetric aptamer based assay for the determination of fluoroquinolones by triggering the reduction-catalyzing activity of gold nanoparticles *Microchim. Acta* **184** 2039
2. Ballesteros O, Toro I, Sanz-Nebot V, Navalón A, Vilchez J L and Barbosa J, 2003 Determination of fluoroquinolones in human urine by liquid chromatography coupled to pneumatically assisted electrospray ionization mass spectrometry *J. Chromatogr. B* **798** 137
3. Gao B, He X-P, Jiang Y, Wei J-T, Suo H and Zhao C 2014 Computational simulation and preparation of fluorescent magnetic molecularly imprinted silica nanospheres for ciprofloxacin or norfloxacin sensing *J. Sep. Sci.* **37** 3753
4. Davis R, Markham A and Balfour J A 1996 Ciprofloxacin *Drugs* **51** 1019
5. Prieto A, Schrader S, Bauer C and Möder M 2011 Synthesis of a molecularly imprinted polymer and its application for microextraction by packed sorbent for the determination of fluoroquinolone related compounds in water *Anal. Chim. Acta* **685** 146
6. Wang B, Jiang Y, Li F and Yang D 2017 Preparation of biochar by simultaneous carbonization, magnetization and activation for norfloxacin removal in water *Bioresour. Technol.* **233** 159
7. Haque M M and Muneer M 2007 Photodegradation of norfloxacin in aqueous suspensions of titanium dioxide *J. Hazard. Mater.* **145** 51
8. Rodríguez E, Navarro-Villoslada F, Benito-Peña E, Marazuela MD and Moreno-Bondi MC 2011 Multiresidue determination of ultratrace levels of fluoroquinolone antimicrobials in drinking and aquaculture water samples by automated online molecularly imprinted solid phase extraction and liquid chromatography *Anal. Chem.* **83** 2046
9. Zhang Q, Jia A, Wan Y, Liu H, Wang K, Peng H, et al. 2014 Occurrences of three classes of antibiotics in a natural river basin: association with antibiotic-resistant *Escherichia coli Environ. Sci. Technol.* **48** 14317
10. Cester C C and Toutain P L 1997 A comprehensive model for enrofloxacin to ciprofloxacin transformation and disposition in dog *J. Pharm. Sci.* **86** 1148
11. Chung H-H, Lee J-B, Chung Y-H and Lee K-G 2009 Analysis of sulfonamide and quinolone antibiotic residues in Korean milk using microbial assays and

high performance liquid chromatography *Food Chem.* **113** 297
12. Lombardo-Agüí M, García-Campaña AM, Gámiz-Gracia L and Cruces Blanco C 2010 Laser induced fluorescence coupled to capillary electrophoresis for the determination of fluoroquinolones in foods of animal origin using molecularly imprinted polymers *J. Chromatogr. A* **1217** 2237
13. Huang K-J, Liu X, Xie W-Z and Yuan H-X 2008 Electrochemical behavior and voltammetric determination of norfloxacin at glassy carbon electrode modified with multi walled carbon nanotubes/Nafion *Colloids Surf. B: Biointerf.* **64** 269
14. Goyal R N, Rana A R S and Chasta H 2012 Electrochemical sensor for the sensitive determination of norfloxacin in human urine and pharmaceuticals *Bioelectrochem.* **83** 46
15. Dang P K, Degand G, Danyi S, Pierret G, Delahaut P, Ton V D, et al. 2010 Validation of a two-plate microbiological method for screening antibiotic residues in shrimp tissue *Anal. Chim. Acta* **672** 30
16. Wu D, Sedgwick A C, Gunnlaugsson T, Akkaya E U, Yoon J and James T D 2017 Fluorescent chemosensors: the past, present and future *Chem. Soc. Rev.* **46** 7105
17. Shanmugaraju S and Mukherjee P S 2015 Self-assembled discrete molecules for sensing nitroaromatics *Chem. Eur. J.* **21** 6656
18. Cook S A and Borovik A S 2015 Molecular designs for controlling the local environments around metal ions *Acc. Chem. Res.* **48** 2407
19. Sk Amanullah, Saha P, Nayek A, Ahmed MdE and Dey A 2021 Biochemical and artificial pathways for the reduction of carbon dioxide, nitrite and the competing proton reduction: effect of 2^{nd} sphere interactions in catalysis *Chem. Soc. Rev.* **50** 3755
20. Shook R L and Borovik A S 2008 The effect of hydrogen bonds on metal-mediated O_2 activation and related processes *Chem. Commun.* **46** 6095
21. Bansal D and Gupta R 2019 Selective sensing of ATP by hydroxide-bridged dizinc(II) complexes offering a hydrogen bonding cavity *Dalton Trans.* **48** 14737
22. Bansal D and Gupta R 2017 Hydroxide-bridged dicopper complexes: the influence of secondary coordination sphere on structure and catecholase activity *Dalton Trans.* **46** 4617
23. Bansal D, Kumar G, Hundal G and Gupta R 2014 Mononuclear complexes of amide-based ligands containing appended functional groups: role of secondary coordination spheres on catalysis *Dalton Trans.* **43** 14865
24. Prabha D, Pachisia S and Gupta R 2021 Cobalt mediated N-alkylation of amines by alcohols: role of hydrogen bonding pocket *Inorg. Chem. Front.* **8** 1599
25. Bansal D and Gupta R 2016 Chemosensors containing appended benzothiazole group(s): selective binding of Cu^{2+} and Zn^{2+} ions by two related receptors *Dalton Trans.* **45** 502
26. CrysAlisPro, v. 1.171.33.49b, Oxford Diffraction Ltd., 2009
27. Altomare A, Cascarano G, Giacovazzo C and Guagliardi A 1993 Completion and refinement of crystal structures with SIR92 *J. Appl. Cryst.* **26** 343
28. Sheldrick G M 2014 *Program for the solution of crystal structures*(University of Gottingen: Gottingen, Germany)
29. Farrugia L J 2003 An integrated system of windows programs for the solution, refinement and analysis of single-crystal X-ray diffraction data, Department of Chemistry, University of Glasgow
30. Kumar V, Kumar P, Kumar S, Singhal D and Gupta R 2019 Turn-on fluorescent sensors for the selective detection of Al^{3+} (and Ga^{3+}) and PPi ions *Inorg. Chem.* **58** 10364
31. Kumar P, Kumar V and Gupta R 2015 Arene-based fluorescent probes for the selective detection of iron *RSC Adv.* **5** 97874
32. Sudheer, Kumar V, Kumar P and Gupta R 2020 Detection of Al^{3+} and Fe^{3+} ions by nitrobenzoxadiazole bearing pyridine-2,6-dicarboxamide based chemosensors: effect of solvents on detection *New. J. Chem.* **44** 13285
33. Kumar S, Kishan R, Kumar P, Pachisia S and Gupta R 2018 Size-selective detection of picric acid by fluorescent palladium macrocycles *Inorg. Chem.* **57** 1693
34. Benesi H A and Hildebrand J H 1949 A spectrophotometric investigation of the interaction of iodine with aromatic hydrocarbons *J. Am. Chem. Soc.* **71** 2703
35. Nakamoto K 2008 *Infrared and Raman spectra of inorganic and coordination compounds: part a: theory and applications in inorganic chemistry* 6th edn. (John Wiley: Hoboken, NJ)
36. Nakamoto K 2008 *Infrared and Raman spectra of inorganic and coordination compounds: part b: applications in coordination, organometallic, and bioinorganic chemistry* 6th edn. (John Wiley: Hoboken, NJ)
37. Geary W J 1971 The use of conductivity measurements in organic solvents for the characterisation of coordination compounds *Coord. Chem. Rev.* **7** 81
38. Reimann M J, Salmon D R, Horton J T, Gier E C and Jefferies L R 2019 Water-soluble sulfonate schiff-base ligands as fluorescent detectors for metal ions in drinking water and biological systems *ACS Omega* **4** 2874
39. Gusev A, Braga E, Zamnius E, Kiskin M, Kryukova M, Baryshnikova A, et al. 2019 Structure and excitation-dependent emission of novel zinc complexes with pyridyltriazoles *RSC Adv.* **9** 22143
40. Rajamanikandan R and Ilanchelian M 2018 Fluorescence sensing approach for high specific detection of 2,4,6-trinitrophenol using bright cyan blue color-emittive poly(vinylpyrrolidone)-supported copper nanoclusters as a fluorophore *ACS Omega* **3** 18251
41. Huang D and Holm R H 2010 Reactions of the terminal $Ni^{II}-OH$ group in substitution and electrophilic reactions with carbon dioxide and other substrates: structural definition of binding modes in an intramolecular NiII···FeII bridged site *J. Am. Chem. Soc.* **132** 4693
42. Donoghue P J, Gupta A K, Boyce D W, Cramer C J and Tolman W B 2010 An anionic, tetragonal copper(II) superoxide complex *J. Am. Chem. Soc.* **132** 15869
43. Donoghue P J, Tehranchi J, Cramer CJ, Sarangi R, Solomon E I and Tolman W B 2011 Rapid C-H bond

activation by a monocopper(III)–hydroxide complex *J. Am. Chem. Soc.* **133** 17602
44. Halvagar M R and Tolman W B 2013 Isolation of a 2-Hydroxytetrahydrofuran Complex From Copper-Promoted Hydroxylation of THF *Inorg. Chem.* **52** 8306
45. Addison A W, Rao T N, Reedijk J, Rijn J van and Verschoor G C 1984 Synthesis, structure, and spectroscopic properties of copper(II) compounds containing nitrogen–sulphur donor ligands; the crystal and molecular structure of aqua[1,7-bis(N-methylbenzimidazol-2′-yl)-2,6-dithiaheptane]copper(II) perchlorate *J. Chem. Soc. Dalton Trans.* 1349
46. Redmore S M, Rickard C E F, Webb S J and Wright L J 1997 Ruthenium complexes of a simple tridentate ligand bearing two "distal" pyridine bases *Inorg. Chem.* **36** 4743
47. Wang D, Lindeman S V and Fiedler A T 2013 Intramolecular hydrogen bonding in Cu^{II} complexes with 2,6-pyridinedicarboxamide ligands: synthesis, structural characterization, and physical properties *Eur. J. Inorg. Chem.* **2013** 4473
48. Pandey S, Kumar P and Gupta R 2018 Polymerization led selective detection and removal of Zn^{2+} and Cd^{2+} ions: isolation of Zn- and Cd-MOFs and reversibility studies *Dalton Trans.* **47** 14686
49. Kumar G, Pachisia S, Kumar P, Kumar V and Gupta R 2019 Zn- and Cd-based coordination polymers offering H-bonding cavities: highly selective sensing of $S_2O_7^{2-}$ and Fe^{3+} ions *Chem. Asian J.* **14** 4594
50. Terenzi A, Lauria A, Almerico A M and Barone G 2015 Zinc complexes as fluorescent chemosensors for nucleic acids: new perspectives for a "boring" element *Dalton Trans.* **44** 3527
51. Kumar P, Kumar V and Gupta R 2017 Detection of the anticoagulant drug warfarin by palladium complexes *Dalton Trans.* **46** 10205
52. Kumar P, Kumar V and Gupta R 2017 Selective fluorescent turn-off sensing of Pd^{2+} ion: applications as paper strips, polystyrene films, and in cell imaging *RSC Adv.* **7** 7734
53. Kumar V, Kumar P and Gupta R 2017 Fluorescent detection of multiple ions by two related chemosensors: structural elucidations and logic gate applications *RSC Adv.* **7** 23127
54. Kumar P, Kumar V, Pandey S and Gupta R 2018 Detection of sulfide ion and gaseous H_2S using a series of pyridine-2,6-dicarboxamide based scaffolds *Dalton Trans.* **47** 9536
55. Ritchie D 2012 Hex Inria; http://hex.loria.fr/
56. Pachisia S and Gupta R 2019 Two Hg(II)-based macrocycles offering hydrogen bonding cavities: influence of cavity structure on heterogeneous catalysis *Cryst. Growth Des.* **19** 6039
57. Hua J, Jiao Y, Wang M and Yang Y 2018 Determination of norfloxacin or ciprofloxacin by carbon dots fluorescence enhancement using magnetic nanoparticles as adsorbent *Microchim. Acta* **185** 137
58. Niu M, Yang X, Ma Y, Hao W, Leng X and Schipper D 2021 Construction of Zn(II)/Cd(II)−Yb(III) schiff base complexes for the NIR luminescent sensing of fluoroquinolone antibiotics *Inorg. Chem.* **60** 5764
59. Gai S, Zhang J, Fan R, Xing K, Chen W, Zhu K, et al. 2020 Highly stable zinc-based meatl-organic frameworks and corresponding flexible composites for removal and detection of antibiotics in water *ACS Appl. Mat. Interf.* **12** 8650